JOURNAL OF APPLIED ELECTROCHEMISTRY 18 (1988) 374–383

Electrochemical behaviour of copper in neutral aerated chloride solution. I. Steady-state investigation

CLAUDE DESLOUIS, BERNARD TRIBOLLET

LP 15 du CNRS 'Physique des Liquides et Electrochimie', associé à l'Université Pierre et Marie Curie, Tour 22, 4 place Jussieu, 75252 Paris Cedex 05, France

GUILIANO MENGOLI, MARCO M. MUSIANI

Istituto di Polarografia ed Elettrochimica Preparativa del CNR, Corso Stati Uniti, 4. 35100 Padova, Italy

Received 10 July 1987; revised 2 October 1987

The electrochemical behaviour of a Cu rotating disc electrode in neutral aerated NaCl solution was investigated in the cathodic and anodic ranges and at the corrosion potential. In the cathodic range, where the reduction of oxygen takes place, reduction peaks allow the identification and quantitative evaluation of insoluble corrosion products (CuCl and Cu_2O). In the anodic range Cu is dissolved, most likely as $CuCl_2^-$. A new mechanism for the anodic dissolution is proposed after comparing our data with previously published mechanisms. Corrosion currents were found to decrease with time and to be a function of the rotation rate of the electrode. Both the mixed kinetics of the anodic partial reaction and diffusion through a porous layer seem to be relevant in controlling I_{corr}.

1. Introduction

Two recent papers described the corrosion of copper in neutral aerated sodium chloride solutions [1, 2]. According to Pourbaix diagrams insoluble corrosion products are expected to form on Cu surfaces at pH > 5.5 [3]. The presence of surface layers introduces additional complexity with respect to Cu corrosion in acidic chlorides where corrosion products are soluble [4–8]. In both Refs [1] and [2] the investigation was restricted to metal–solution interaction times so short that an oxide-free surface could be assumed. This assumption enabled Dhar *et al.* [2] to apply the kinetic model developed by Smyrl for the corrosion of Cu in acidic environments [7].

From a practical point of view, the corrosion behaviour of Cu after a long interaction time with the medium, i.e. once the metal is covered by corrosion products, is of much greater interest. Surface layers may influence the development of corrosion phenomena in many ways, e.g. they may partially block the metal surface or may influence the mass transfer of either oxygen or oxidized Cu species (or both). Indeed mass transfer was claimed to affect both the anodic and the cathodic partial reactions [9]:

$$Cu + 2Cl^- \longrightarrow CuCl_2^- + e^- \quad \text{(anodic)}$$

$$O_2 + 2H_2O + 4e^- \longrightarrow 4OH^- \quad \text{(cathodic)}$$

The diffusion control in the electrodissolution of Cu was ascribed by different authors either to Cl^- transport to the surface [10] or to the transport of $CuCl_2^-$ to the bulk solution [11–16].

Although much work was devoted to the chemical identification of the corrosion products formed at Cu in various media and to their physical characterization [17], a correlation among the amount of surface oxides, mass transfer and corrosion currents was not generally attempted. (Loss and Heitz [9] discussed Cu erosion–corrosion in terms of mechanically stimulated electrochemical breakdown of a passivating oxide film, but the amounts of surface oxides were not determined.)

In the present and the following papers we attempt to assess the corrosion behaviour of Cu in neutral and aerated sodium chloride solutions once the metal is covered by a corrosion product layer. Steady-state experiments are combined with transient a.c. and electrohydrodynamical (EHD) impedance techniques. The former were used initially for determining corrosion currents and Cu coverage by corrosion products and eventually for obtaining some knowledge on mass transport involved in the partial reactions; a.c. and EHD impedance techniques were then used in order to investigate the corrosion and mass transfer mechanisms more thoroughly. The results of the impedance experiments are described in Part II.

2. Experimental details

Copper disc electrodes (prepared from Carlo Erba 99.999% copper) had an area of 0.196 cm^2. Either Teflon or Plexyglass, the latter in combination with an epoxy resin, were used as sheath materials. The electrodes were polished by using alumina powder (ϕ = 5–0.03 μm).

Solutions were prepared using distilled water and analytical grade NaCl. Either single-compartment cells or cells with a separate compartment for the reference electrode (saturated calomel electrode, SCE) were used.

An AMEL 553 potentiostat, an AMEL 568 programmable function generator and an AMEL 731 integrator were used for all voltammetric and coulo-

0021-891X/88 $03.00 + .12

metric experiments. Current–potential curves were recorded both in the anodic and cathodic directions, starting from the corrosion potential, after leaving the electrode stationary at open circuit for variable times. Variable rotation rates and a 0.5 mV s^{-1} scan rate were used.

Cyclic voltammograms over a 10-mV range, centred at the corrosion potential, were recorded at different rotation rates with a 0.1 mV s^{-1} scan rate, after rest times spent either under rotation or stationary. The polarization resistance (R_p) was then determined from the slope of the tangent to the current–potential curve at the corrosion potential.

The amount of insoluble corrosion products formed on the electrode surface during exposure to the test solutions was measured by submitting the Cu electrode to the following sequence of potentials: −250/−1250/−600/−1250/−600 mV vs SCE. Coulometric measurements were carried out at a scan rate of 5 mV s^{-1} after purging the NaCl solution with N_2. The difference between the charge integrated in the first half sequence (−250/−1250/−600) and that integrated in the second half (−600/−1250/−600) was associated with the reduction of surface layers. The above potential limits were chosen because −250 mV is very close to E_{corr} (corrosion potential) and the current became negligible at −600 mV in the sweeps towards positive potential.

All experiments were carried out at room temperatures (20–25° C). Although some influence of illumination on the growth of oxides at Cu surfaces was observed [18] this parameter was not controlled in our experiments. Long rest times involved an alternation of dark and light periods.

3. Results

3.1. *Current–potential curves*

Current–potential curves for Cu in aerated 0.5 M NaCl were recorded after various exposure times (5 min, 1 h, 16 h at open circuit) at 300, 1000 and 3000 rpm starting from the corrosion potential. They display a dependence on the rotation rate of the electrode for both the cathodic and the anodic branches (Fig. 1).

3.2. *Cathodic curves*

The shape of the cathodic polarization curves depends strongly on the time of immersion in aerated 0.5 M NaCl. Log I vs E plots obtained at 1000 rpm after 5 min and 16 h immersion in aerated 0.5 M NaCl are compared in Fig. 2. For the shorter immersion time (dashed curve) a peak is seen at $E = -410$ mV, which perturbates the linear region. A cathodic plateau is then observed between −750 and −1150 mV, due to O_2 reduction. The position of the peak is somewhat irreproducible and is found to change in the range −320 to −450 mV depending on the rotation rate. The charge associated with this peak is in the range 15–30 mC cm^{-2}, corresponding to an average thickness of 50–100 monolayers (if the electrode is assumed

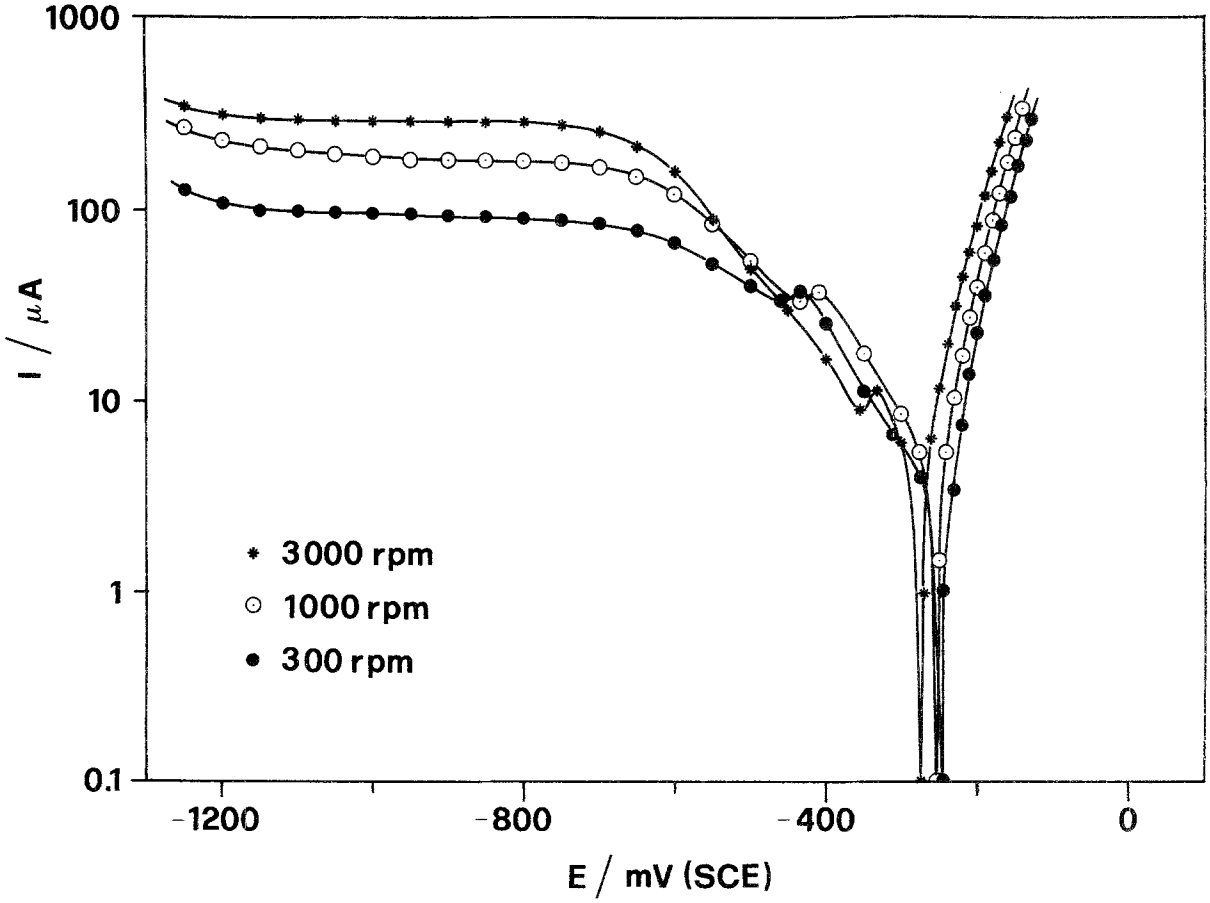

Fig. 1. Current–potential curves for Cu in aerated 0.5 M NaCl recorded after 5 min at E_{corr}. Scan rate = 0.5 mV s^{-1}.

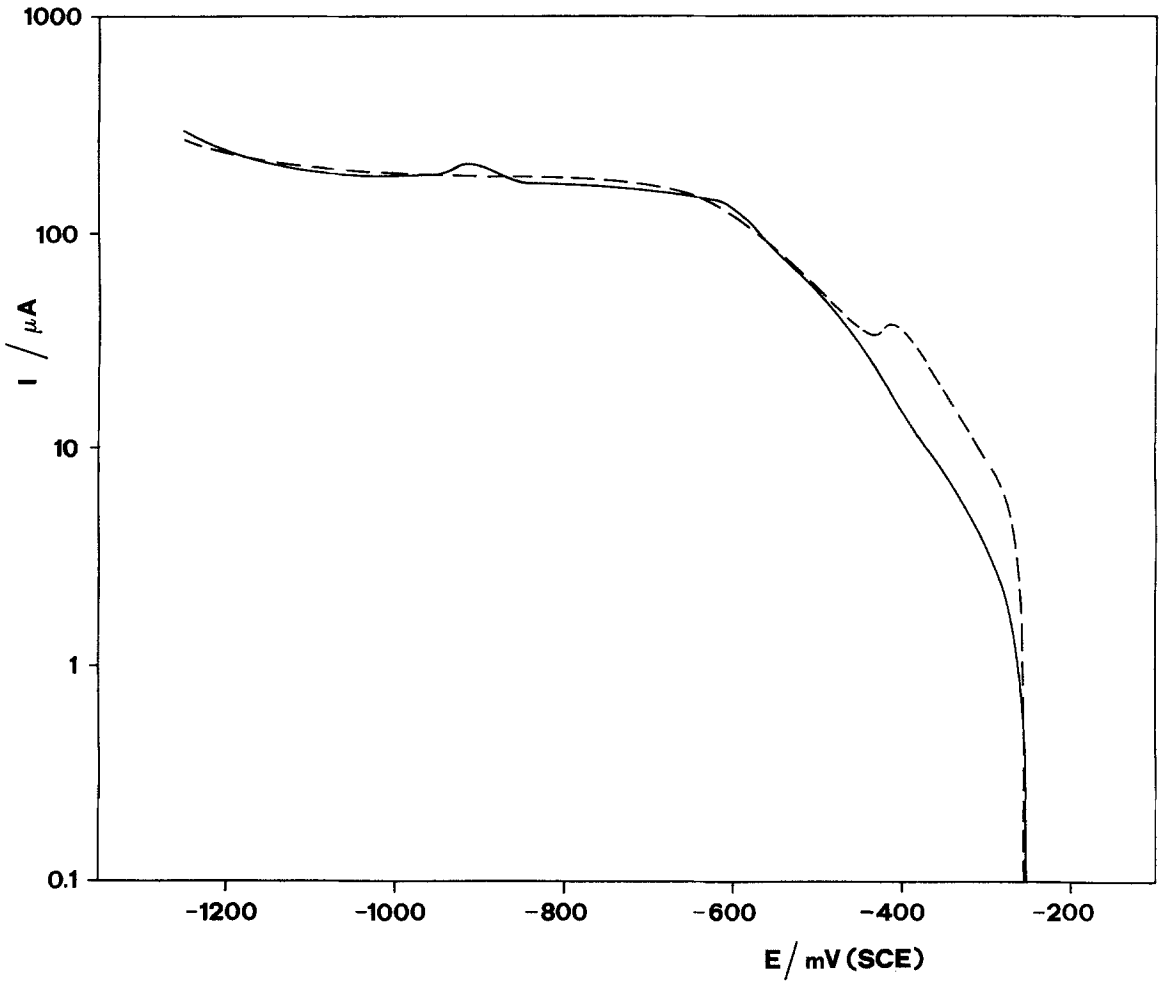

Fig. 2. Comparison of the cathodic current–potential curves recorded at Cu in aerated 0.5 M NaCl after 5 min (– – –) and 16 h (——) at E_{corr}. Scan rate = 0.5 mV s^{-1}. Ω = 1000 rpm.

to be ideally flat and one electron is involved in the corresponding reaction). In more dilute solutions (0.1 M) at all rotation rates, a very pronounced peak is found at values of E between −250 and −350 mV. Conversely in 5 M NaCl no peak is detected in the cathodic region. In agreement with Nobe, who identified the primary oxidation product as CuCl on the basis of thermodynamic considerations [1], and with Moreau [14] who analysed the electrode surface by X-ray diffraction, we ascribe this cathodic peak to CuCl reduction. It is not found in 5 M NaCl because at higher chloride concentration the equilibrium

$$CuCl + Cl^- \rightleftharpoons CuCl_2^-$$

is shifted towards the soluble Cu complexes.

After a 16-h immersion (solid curve in Fig. 2) a reduction peak is found at −900 mV, superimposed to the diffusion-limited current of O_2 reduction, and no other peak is present. The potential of this peak is in agreement with the reduction of Cu_2O [19, 20], formed by hydrolysis of the primary cuprous corrosion products. Further support to this identification is offered by the photoreduction current seen in the first cycle before the reduction peak, in agreement with the p-type semiconducting properties of Cu_2O [17]. The dependence of the amount of Cu_2O on immersion time and Ω will be dealt with in the next section.

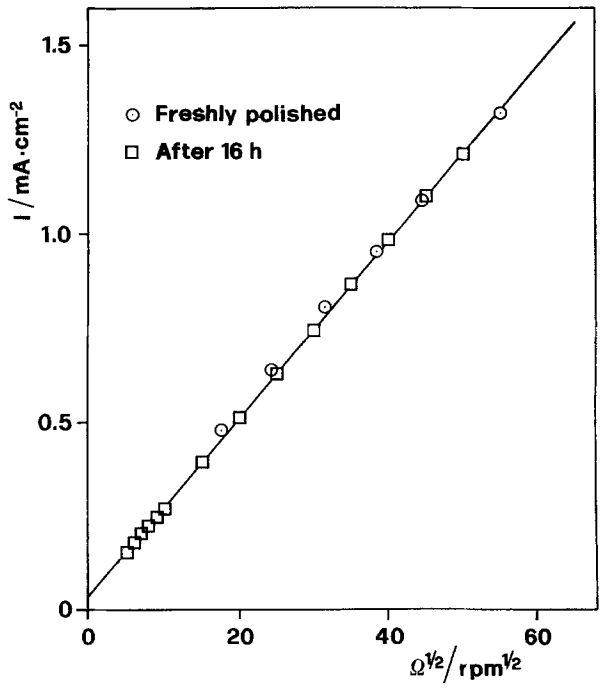

Fig. 3. Cathodic limiting currents recorded at −800 mV (SCE) on a Cu electrode either freshly polished (○) or after 16 h immersion in aerated 0.5 M NaCl (□).

A lack of influence of the corrosion product layer on O_2 diffusion can be anticipated from Fig. 2 since the height of the cathodic plateau is independent of immersion time. A linear dependence of I on $\Omega^{1/2}$ is observed (Fig. 3) at -800 mV for both a freshly polished electrode or after 16 h at E_{corr}. Although Cu_2O formed on the latter is not reduced at this potential, the two sets of points are very close to each other, i.e. a Cu_2O-coated electrode behaves as bare Cu with respect to O_2 reduction. From the slope of the I vs $\Omega^{1/2}$ line the diffusion coefficient for oxygen may be calculated according to the Levich relation for a uniformly accessible electrode; it becomes 2×10^{-5} cm^{2}s^{-1} with $n = 4$ and 5.6×10^{-5} with $n = 2$, by assuming $c_\infty = 2 \times 10^{-7}$ mol cm^{-3} and $\nu = 0.89 \times 10^{+2}$ cm^{-2}s^{-1}. The value 2×10^{-5} cm^{2}s^{-1}, corresponding to $n = 4$, is in agreement with that found in the same medium on an Fe electrode [21].

The cathodic current measured between E_{corr} and -500 mV after a rest time at open circuit was found to respond with slow, rather irreproducible transients to variations of Ω; the behaviour in this potential region studied by EHD impedance is described in Part II.

3.3. *Coulometry of Cu_2O*

The charge consumed for the reduction of Cu_2O formed on a stationary Cu electrode was found to increase markedly with the time of immersion in 0.5 M NaCl: it was 8.5 mC cm^{-2} after 3 h, 62 mC cm^{-2} after 16 h and 158 mC cm^{-2} after 88 h. It may be calculated that about 0.3 mC cm^{-2} are necessary to oxidize a Cu monolayer to Cu^+ ($\sim 3.2 \times 10^{-9}$ moles cm^{-2}), i.e. the charge consumed for the longest immersion time corresponds to about 500 monolayers. The dependence of the amount of Cu_2O formed during a 16 h exposure under continuous stirring on Ω is described in Fig. 4. A slow rotation rate (300 rpm) constantly applied is sufficient to cause a drop in the reduction charge, which does not markedly decrease further by increasing Ω until 3000 rpm. Rotation of the electrode, by favouring $CuCl_2^-$ diffusion towards the bulk solution, is likely to decrease the surface amount of primary corrosion products and prevent extensive local hydrolysis to Cu_2O. The reduction charges measured at Cu electrodes left stationary for 15 h at open circuit and then kept 1 additional hour at Ω ranging from 0 to 3000 rpm is almost constant for $\Omega < 1000$ rpm but decreases significantly at higher Ω, see Fig. 4. Thus, high rotation rates, $\Omega > 1000$ rpm, seem to cause also some erosion of the Cu_2O surface layers already formed.

3.4. *Anodic curves*

Linear Tafel regions with slopes close to 60 mV (current decade)$^{-1}$ [10, 12–16] may be identified for all anodic curves recorded in 0.5 M NaCl which become less sensitive to the hydrodynamic conditions at longer exposure times. Cu dissolution currents are higher at 1 h than 5 min exposure and then decline.

The dependence of the dissolution current of Cu on Ω was investigated at various potentials in NaCl solutions, the concentrations of which were in the range from 0.1 to 1.5 M. I vs $\Omega^{1/2}$ plots show a curvature and negligible non-diffusional components, while reciprocal plots (I^{-1} vs $\Omega^{-1/2}$) are straight lines with positive intercepts on the ordinate axis. Figure 5 shows, for instance, I^{-1} vs $\Omega^{-1/2}$ plots obtained for various combinations of [Cl^-] and potential. The best fit values for I_∞ and the slope ($dI^{-1}/d\Omega^{-1/2}$) are summarized in Table 1 as a function of potential and [Cl^-].

Plots of ($dI^{-1}/d\Omega^{-1/2}$) vs E, Fig. 6, and I_∞ vs E, Fig. 7, are straight lines, in semilog coordinates, in agreement with Smyrl [8]. The slope of the plots in Fig. 6 varies between 60 and 70 mV decade^{-1}, being

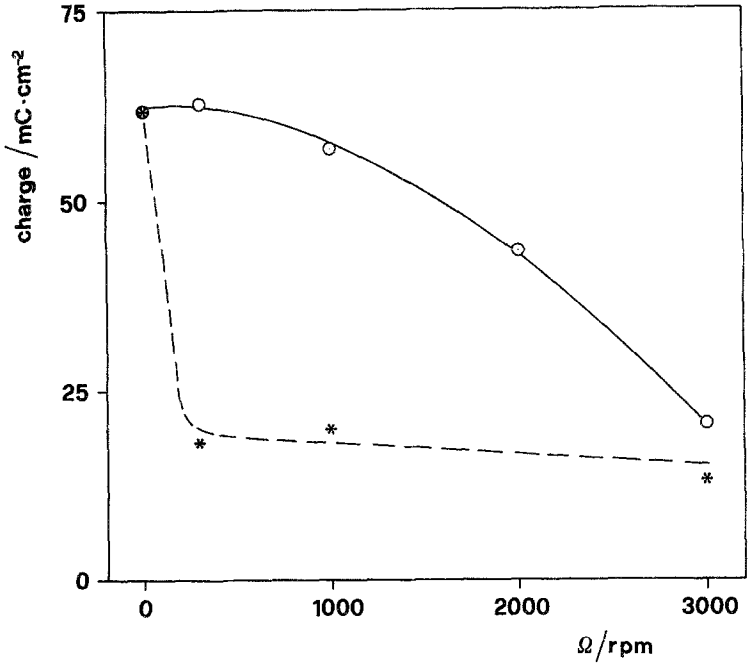

Fig. 4. Charge consumed for the reduction of Cu_2O formed on a Cu electrode after 16 h exposure to aerated 0.5 M NaCl either under continuous rotation (*) or with rotation only during the last hour (○).

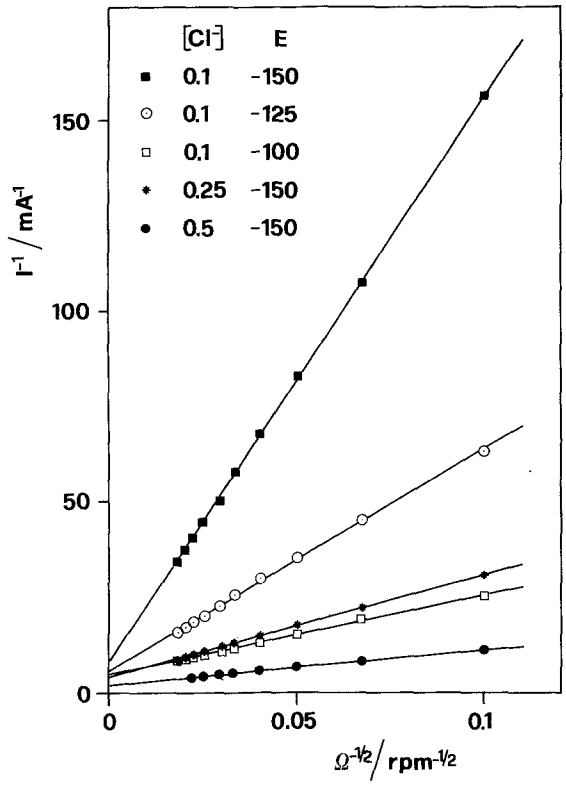

Fig. 5. Anodic I^{-1} vs $\Omega^{-1/2}$ plots obtained on Cu for various combinations of potential and [Cl^-].

higher for the higher chloride concentrations. In Fig. 7, decreasing slopes from 220 to 170 mV decade^{-1} are found for increasing concentrations of chloride. I_∞ and $dI^{-1}/d\Omega^{-1/2}$ also depend on [Cl^-], as shown in Fig. 8; log I_∞ and log ($dI^{-1}/d\Omega^{-1/2}$) vs log [Cl^-] have slopes slightly lower than 1 and slightly less negative than -2, respectively.

3.5. *Polarization resistance–corrosion current*

Polarization resistance values (R_p) obtained for various Ω and two exposure times are reported in Fig. 9. For each exposure time (1 h or 16 h) two sets of data are reported. The empty points refer to experiments where the electrode was continuously rotated during the rest time at $E = E_{corr}$ at the same Ω where R_p was measured (procedure A), while full points were obtained by leaving the electrode stationary during the rest time and rotating it only for the short time necessary to achieve a stable E_{corr} before the measurement (procedure B). In both instances the electrode was polished before each experimental point. The latter procedure is expected to minimize the influence of rotation rate on the amount of insoluble corrosion products. The plots of R_p vs $\Omega^{-1/2}$ in Fig. 9 yield straight lines with positive intercepts on the ordinate axis. The extrapolated value of R_p at $\Omega = \infty$, $R_{p\infty}$, and the slopes are reported in Table 2.

Table 1. Best-fit values of the extrapolated current at infinite rotation and the slope of I^{-1} vs $\Omega^{-1/2}$ for the electrodissolution of Cu

E (mV)	[Cl^-]	I_∞ (μA)	*Slope* ($\mu A^{-1}\ rpm^{1/2}$)
−150	0.1	132	1.50
−125	0.1	172	0.580
−100	0.1	204	0.207
−75	0.1	286	0.0887
−175	0.25	196	0.668
−150	0.25	256	0.277
−100	0.25	500	0.0456
−75	0.25	833	0.0199
−225	0.5	137	1.066
−200	0.5	213	0.463
−150	0.5	400	0.0892
−225	1.5	294	0.163
−200	1.5	454	0.0701
−150	1.5	909	0.0133

The common technique of determining the corrosion current from R_p [22] was found by Grubitsch *et al.* [23] to yield, for the Cu/seawater system, results in agreement with weight loss measurements, provided no pitting occurs. Grubitsch [23] and later Heitz [9] calculated I_{corr} as $I_{corr} = B/R_p$, with $B = 0.019$ V. The numerical value of the constant B was obtained by assuming a pure activation mechanism for both the anodic and the cathodic reactions. This corresponds

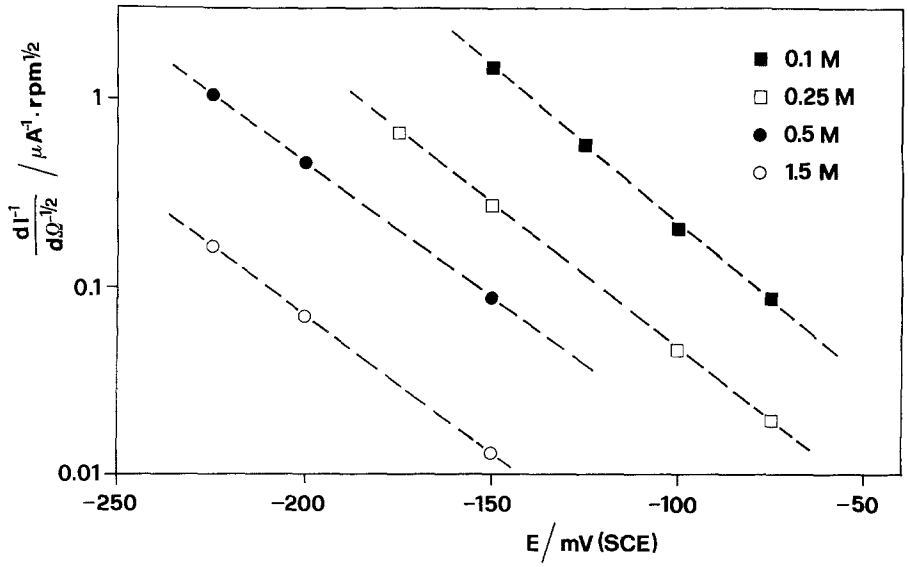

Fig. 6. Dependence of the slope ($dI^{-1}/d\Omega^{-1/2}$) on potential.

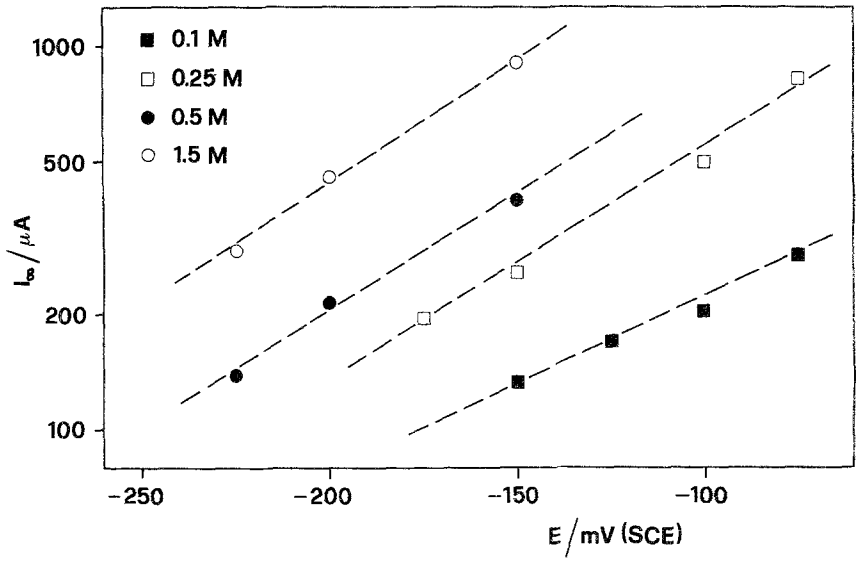

Fig. 7. Dependence of the extrapolated current at infinite rotation, I_∞, on potential.

to the assumption that R_p coincides with R_t, which is at variance with our experimental results. However, we will show in the following discussion that according to our results and to the mechanism proposed for the anodic dissolution of Cu, in this particular instance, I_{corr} is indeed proportional to $1/R_p$ and the same value for B is obtained. Thus, we calculated I_{corr} as $0.019/R_p$ and plotted the values vs $\Omega^{1/2}$ (Fig. 10).

Corrosion currents decrease significantly by prolonging the immersion time and are higher for procedure A than for procedure B (by a factor of 1.4–1.7). By comparing the corrosion currents and coulometry of Cu_2O and assuming a linear variation of I_{corr} from the beginning of the exposure to 16 h, it may be estimated that, after 16 h, 20–25% of the corroded copper is converted to Cu_2O. If the concentration of NaCl is reduced to 0.1 M, the insoluble fraction reaches 60%.

3.6. *Corrosion potential*

The corrosion potential of a Cu disc electrode, either stationary or rotating, in aerated 0.5 M NaCl solution, after an initial cathodic shift during the first hour, becomes less negative for longer exposure times. For exposure times between 16 and 90 h, increasing rotation rates correspond to more negative corrosion potentials. E_{corr} varies by 15 mV per decade of Ω (compare [2]), though its value is not fully reproducible in different experiments. This behaviour suggests that the anodic partial reaction is more strongly affected by mass transport than the cathodic one. The change in the sign of $dE_{corr}/d\Omega$ after long exposures described by Heitz *et al.* [9] and ascribed to a prevailing effect of rotation on O_2 transport was not detected in the present study. However, Fig. 11 shows that stepping the rotation rate from 0 to 1000 rpm produces markedly different effects on E_{corr} at short (5 min, curve a) and long (88 h, curve b) immersion times. The corrosion potential of a freshly immersed electrode steadily shifts towards negative values. Conversely, after a long immersion, the initial shift is toward positive potential and only after 2 min this trend is reversed.

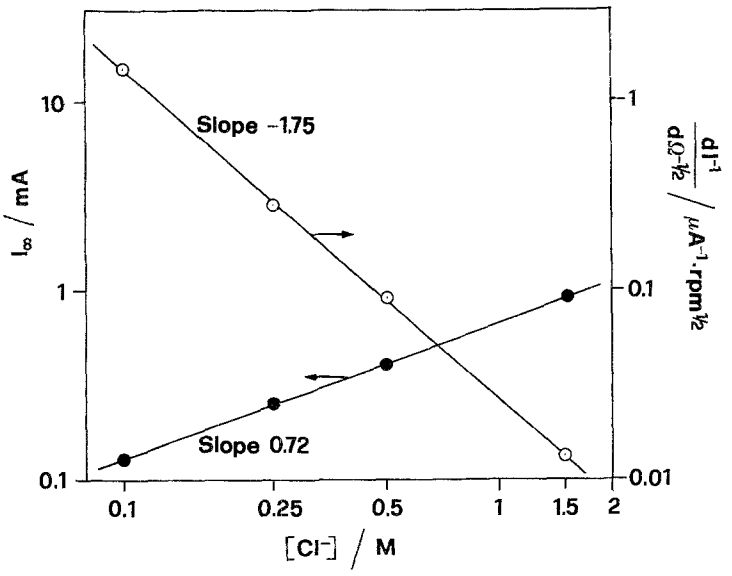

Fig. 8. Dependence of the slope ($dI^{-1}/d\Omega^{-1/2}$) and extrapolated current at infinite rotation, I_∞, on $[Cl^-]$.

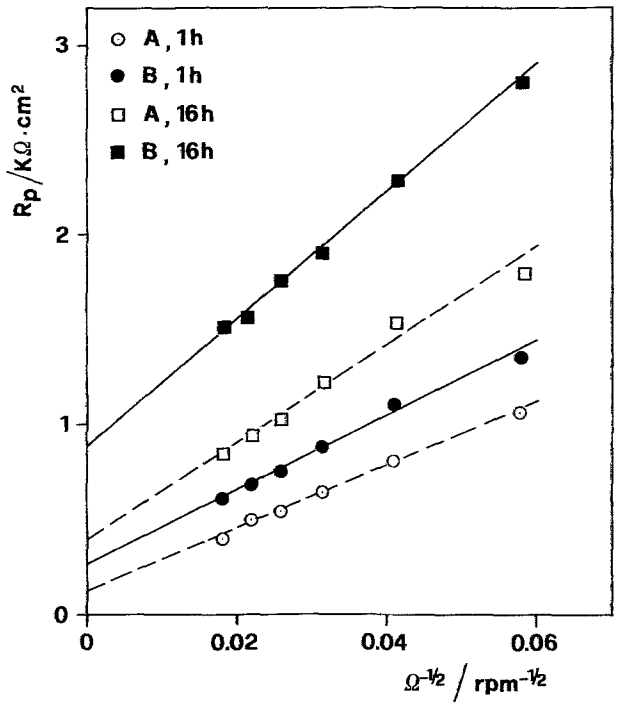

Fig. 9. Polarization resistance (per unit area) of Cu in aerated 0.5 M NaCl as a function of rotation rate and immersion time.

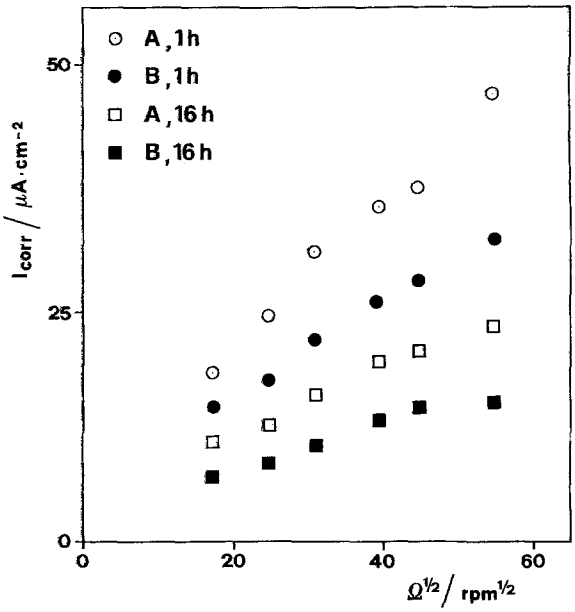

Fig. 10. Corrosion current densities of Cu in aerated 0.5 M NaCl as a function of rotation rate and immersion time.

4. Discussion

4.1. *Electrodissolution*

The kinetics and mechanisms of the anodic dissolution of copper in chloride solutions have been studied by many authors [8, 10–16, 24]. Most experimental data correspond to acidic media but, since Cu electrodissolution was found to be essentially independent of pH [16], the various mechanisms proposed can be applied for both acidic and neutral solutions. Copper dissolves anodically in chloride media to form $CuCl_2^-$ at low current densities and at sufficiently low chloride concentrations (< 1 M [8]).

The first model, developed by Bacarella and Griess [12] in 1973, considers the global reaction:

$$Cu + 2Cl^- \rightleftharpoons CuCl_2^- + e^- \qquad (1)$$

The oxidation of Cu to $CuCl_2^-$ was assumed to be in equilibrium so that the Nernst equation is applicable. The steady flux of $CuCl_2^-$ at the surface is related to the current:

$$i = FD[CuCl_2^-]/\delta \qquad (2)$$

The expression for current was obtained as:

$$i/F = (D/\delta)[Cl^-]^2 \exp(FE/RT) \qquad (3)$$

Table 2. Best-fit values for the extrapolation at infinite rotation and the slope of R_p vs $\Omega^{-1/2}$ plots for Cu in aerated 0.5 M NaCl

Experiment	$R_{p\infty}$ (Ωcm^2)	*Slope* ($\Omega cm^2\ rpm^{1/2}$)
1 h, A	120	16 500
1 h, B	264	19 350
16 h, A	405	25 050
16 h, B	879	33 600

Recently Tribollet and Newman [24] also considered the global reaction but used the general kinetic equation

$$i/F = k_a[Cl^-]^2 \exp(\alpha FE/RT) - k_c[CuCl_2^-] \exp(-(1-\alpha)FE/RT) \qquad (4)$$

By combining this equation with equation (2) they obtained:

$$i/F = \{k_a[Cl^-]^2 \exp(\alpha FE/RT)\}/\{1 + (\delta/D)k_c \times \exp(-(1-\alpha)FE/RT)\} \qquad (5)$$

In contrast, Moreau *et al.* [14] and also Lee and Nobe [16] considered that the anodic reaction can be represented by a two-step sequence

$$Cu + Cl^- \underset{k_{-1}}{\overset{k_1}{\rightleftharpoons}} CuCl + e^- \qquad (6)$$

$$CuCl + Cl^- \underset{k_{-2}}{\overset{k_2}{\rightleftharpoons}} CuCl_2^- \qquad (7)$$

The first reaction was assumed to be fast and at quasi-equilibrium, so that

$$k_1[Cl^-] \exp(FE/RT) = k_{-1}[CuCl] \qquad (8)$$

With the usual Equation 2, they obtained

$$i/F = \{(k_2k_1/k_{-1})[Cl^-]^2 \times \exp(FE/RT)\}/\{1 + (\delta/D)k_{-2}\} \qquad (9)$$

According to Smyrl [8], copper dissolves anodically in acidic chloride by the one-electron reaction

$$Cu \rightleftharpoons Cu^+ + e^- \qquad (10)$$

The cuprous species also participate in a complexation reaction whose equilibrium constant is

$$K_c = [CuCl_2^-]/[Cu^+][Cl^-]^2 = 6.96 \times 10^4 \qquad (11)$$

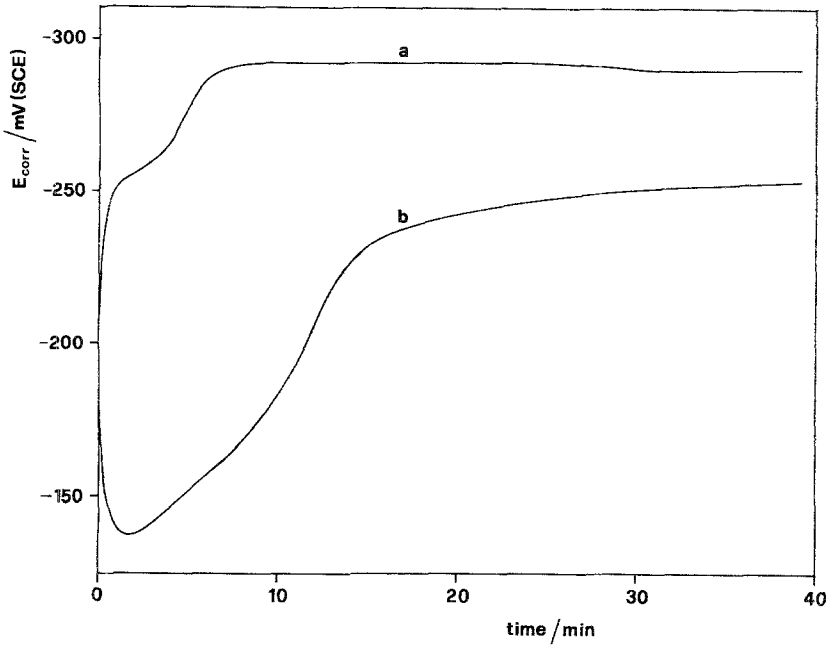

Fig. 11. Evolution of E_{corr} with time after changing Ω from 0 to 1000 rpm. Rest time at $\Omega = 0$: 5 min (a) and 88 h (b).

By using the kinetic equation corresponding to the electrochemical reaction (10), with the relations (11) and (2), Smyrl obtained

$$i/F = \{k_a \exp(\alpha_a FE/RT)\}/\{1 + (k_c\delta/k_a[Cl^-]^2 D) \times \exp(-(\alpha_c FE/RT)\} \quad (12)$$

Thus, these four different models yield four different expressions for the current, which may be compared with our experimental results. Our, and all recent experimental data [1, 8, 16], show a dependence of the current on the rotation rate following the equation

$$I^{-1} = I_\infty^{-1} + \gamma\Omega^{-1/2} \quad (13)$$

Only the first model [12] (Equation 3) fails to agree with this relationship while the other three follow Equation 13. We now compare the dependence of I_∞ and γ on potential and chloride concentration. All three models give a dependence of γ on potential of 60 mV decade^{-1} and on $[Cl^-]^2$, in relative good agreement with the published experimental data [8, 16] and our results (Figs 6 and 8). The difference among these three models appears only on I_∞. The dependence of I_∞ on potential and chloride concentration is summarized in Table 3.

Table 3. Dependence of I_∞ on potential and chloride concentration according to mechanisms proposed in the literature

Authors	*Dependence on E*	*Dependence on $[Cl^-]$*
Tribollet and Newman [24] Equation 5	120 mV decade^{-1} with $\alpha = 0.5$	$[Cl^-]^2$
Moreau *et al.* [14] Lee and Nobe [16] Equation 9	60 mV decade^{-1}	$[Cl^-]^2$
Smyrl [8] Equation 12	120 mV decade^{-1} with $\alpha = 0.5$	independent

Smyrl found a slope of log I_∞ vs V of 120 mV decade^{-1} in agreement with both his own mechanism and that of Tribollet and Newman. In the present study we found larger values which can also be explained with the above models if α is < 0.5. We have shown in this paper (Fig. 9) an almost linear dependence of I_∞ on chloride concentration, in disagreement with all models. Thus, we were prompted to propose a new model.

We consider again, as Moreau *et al.* [14] and Lee and Nobe [16], the two-step sequence given by Equations 6 and 7 but we do not assume the first reaction at quasi-equilibrium. Then:

$$i/F = k_1[Cl^-]\exp(\alpha FE/RT) - k_{-1}[CuCl]\exp(-(1-\alpha)FE/RT) \quad (14)$$

Mass balance gives:

$$d[CuCl]/dt = k_1[Cl^-]\exp(\alpha FE/RT) - k_{-1}[CuCl] \times \exp(-(1-\alpha)FE/RT) + k_{-2}[CuCl_2^-] - k_2[CuCl][Cl^-] \quad (15)$$

$CuCl_2^-$ diffuses from the surface according to the usual Equation 2. The steady-state solution of this set of three Equations 2, 14 and 15 is obtained for $d[CuCl]/dt = 0$

$$F/i = 1/\{k_1[Cl^-]\exp(\alpha FE/RT)\} + k_{-1}\exp(-FE/RT)/k_1k_2[Cl^-]^2 + k_{-1}k_{-2}\delta\exp(-FE/RT)/k_1k_2[Cl^-]^2 D \quad (16)$$

With this model, the expression for $(dI^{-1}/d\Omega^{-1/2})$ is analogous to the previous ones and in relatively good agreement with all the experimental data.

At high anodic overpotentials the term

$1/k_1[Cl^-]\exp(\alpha FE/RT)$ of the I_∞ expression Equation 16 is predominant and a linear dependence on chloride concentration is expected in relatively good agreement with our experimental data (Fig. 9). (If chloride ion activity, $a(Cl^-)$, is used instead of its concentration, the slope of the log I vs log $a(Cl^-)$ plot becomes 0.84.) In the same way, the potential dependence of I_∞ is 120 mV decade^{-1} or more if $\alpha < 0.5$, in agreement with experimental data.

4.2. *Corrosion*

The formula derived for anodic dissolution (16) may be used for the calculation of I_{corr}. At the corrosion potential, as a first approximation, $1/I_\infty$ may be neglected and the anodic current may be written from Equation 16 as

$$I_a = FK_a\Omega^{1/2}\exp(FE/RT)$$

with

$$K_a = k_1k_2[Cl^-]^2D^{2/3}\nu^{-1/6}/1.8\,k_{-1}k_{-2} \quad (17)$$

From the current–potential curves of Fig. 1, the cathodic current varies with potential with a slope of -180 mV decade^{-1}, so by assuming that at the corrosion potential the oxygen reduction is purely kinetic

$$I_c = -FK_c\exp(-FE/3RT) \quad (18)$$

At E_{corr} the polarization resistance is

$$1/R_p = 1/R_{pa} + 1/R_{tc} \quad (19)$$

$$1/R_p = (F/RT)I_a - (F/3RT)I_c \quad (20)$$

since $I_{corr} = I_a = -I_c$

$$R_p = B/I_{corr} \text{ with } B = 3RT/4F = 0.019\,V \quad (21)$$

This calculation yields the same numerical value for B as that of Grubitsch [23] because R_{pa} depends exponentially on E.

From Equations 17 and 18 it is easy to obtain the variation of the corrosion potential with the rotation rate

$$V_2 - V_1 = (0.019/2)\log(\Omega_1/\Omega_2) \quad (22)$$

In agreement with previous investigations [1, 2] and our model (Equations 20–22), our results indicate that the corrosion of copper in neutral aerated NaCl solution is a function of the rotation rate of the electrode, Fig. 9. The values of extrapolated R_p at infinite rotation, $R_{p\infty}$, in Fig. 9 may either indicate a mixed control of I_{corr} or diffusion through a surface layer. The presence of such a layer is demonstrated by the cathodic polarization curves. At immersion times higher than 1 h, the layer consists mainly of Cu_2O formed by hydrolysis of a Cu(I) species. The hydrolytic reaction is competitive with the complexation of CuCl by Cl^- and the removal of the produced $CuCl_2^-$ by mass transfer. This interpretation is in agreement with the dependence of the charge consumed for the reduction of Cu_2O on Ω. It also explains why $R_{p\infty}$ increases with the time of immersion and is higher for procedure B than for procedure A.

The slope of the straight lines in Fig. 9 is also higher for procedure B than for procedure A and increases with the time of immersion (i.e. it is higher when the corrosion potential is less negative). Since the diffusion through a layer would only change $R_{p\infty}$ but not the slope, the change in the slope is explained as a result of the mixed control of the anodic partial reaction, as described above. However, an effect by a layer is not ruled out since it is additive to that of a slow kinetics.

Equation 22 corresponds to a variation of E_{corr} of 22 mV decade^{-1} of Ω in fair agreement with our experimental data and Ref. [2]. The bad reproducibility of E_{corr} and the discrepancy between the model and experimental data may be due to the properties (thickness and perhaps morphology) of the Cu_2O layer.

Steady-state techniques do not allow full elucidation of the link between mass transfer and the corrosion of copper. A complete assessment of the effect of surface layers on cathodic and anodic mass transfer cannot be achieved by steady-state experiments. Although it has been clearly established that Cu_2O does not interfere with O_2 reduction on the cathodic plateau, at less negative potentials, where some CuCl is also likely to be present, the cathodic partial reaction (assumed, so far, to be purely kinetic at E_{corr}) could be controlled by diffusion through a layer. Impedance techniques were used with the aim of better clarifying these points and further checking the proposed model. The results are described in Part II.

Acknowledgement

The authors thank Mr F. Furlanetto of Italian CNR for valuable experimental work.

References

[1] W. D. Bjorndahl and K. Nobe, *Corrosion* **40** (1984) 82.
[2] H. P. Dhar, R. E. White, G. Burnell, L. R. Cornwell, R. B. Griffin and R. Darby, *Corrosion* **41** (1985) 317.
[3] G. Bianchi and P. Longhi, *Corros. Sci.* **13** (1973) 853.
[4] B. Miller and M. I. Bellavance, *J. Electrochem. Soc.* **119** (1972) 1510.
[5] G. Faita, G. Fiori and D. Salvadore, *Corros. Sci.* **15** (1975) 383.
[6] W. H. Smyrl, in 'Electrochemical Corrosion Testing' (edited by F. Mansfeld and U. Bertocci), ASTM, Philadelphia (1981) p. 198.
[7] W. H. Smyrl, in 'Comprehensive Treatise of Electrochemistry' (edited by J. O'M Bockris, B. E. Conway, E. Yeager and R. E. White) Plenum, New York (1981) Vol. 4, p. 97.
[8] W. H. Smyrl, *J. Electrochem. Soc.* **132** (1985) 1556, 1563.
[9] C. Loss and E. Heitz, *Werkst. Korros.* **24** (1973) 38.
[10] M. Braun and K. Nobe, *J. Electrochem. Soc.* **126** (1979) 1666.
[11] T. Hurlen, *Acta Chem. Scand.* **15** (1961) 1231.
[12] A. L. Bacarella and J. C. Griess, *J. Electrochem. Soc.* **120** (1973) 459.
[13] C. H. Bonfiglio, C. H. Albaya and O. A. Cobo, *Corros. Sci.* **13** (1973) 717.
[14] A. Moreau, *Electrochim. Acta* **26** (1981) 1609; A. Moreau, J. P. Frayret, F. Del Rey and R. Pointeau, *ibid.* **27** (1982) 1281.

[15] L. Brossard, *J. Electrochem. Soc.* **130** (1983) 403.
[16] H. P. Lee and K. Nobe, *J. Electrochem. Soc.* **133** (1986) 2035.
[17] F. Di Quarto, S. Piazza and C. Sunseri, *Electrochim. Acta* **30** (1985) 315 and references cited therein.
[18] U. Bertocci, in 'Encyclopedia of Electrochemistry of the Elements' (edited by A. J. Bard), Marcel Dekker, New York (1974) Vol. II, p. 383.
[19] C. Fiaud, *Corros. Sci.* **14** (1974) 261.
[20] L. M. Abrantes, L. M. Castillo, C. Norman and L. M. Peter, *J. Electroanal. Chem.* **163** (1984) 209.
[21] A. Bonnel, F. Dabosi, C. Deslouis, M. Duprat, M. Keddam and B. Tribollet, *J. Electrochem. Soc.* **130** (1983) 753.
[22] F. Mansfeld, in 'Advances in Corrosion Science and Technology' (edited by M. G. Fontana and R. W. Staehle), Plenum, New York (1978) Vol. 8, p. 163.
[23] H. Grubitsch, F. Hilbert and R. Sammer, *Werkst. Korros.* **17** (1966) 760.
[24] B. Tribollet and J. Newman, *J. Electrochem. Soc.* **131** (1984) 2780.